Constitutive Model for Fiber-Reinforced Composite Laminates

Bibiana M. Luccioni
CONICET,
Structures Institute,
National University of Tucumán,
Av. Roca 1800,
4000 San Miguel de Tucumán,
Tucumán, Argentina

Nowadays, conventional materials have been progressively replaced by composite materials in a wide variety of applications. Particularly, fiber reinforced composite laminates are widely used. The appropriate design of elements made of this type of material requires the use of constitutive models capable of estimating their stiffness and strength. A general constitutive model for fiber reinforced laminated composites is presented in this paper. The model is obtained as a generalization of classical mixture theory taking into account the relations among the strains and stresses in the components and the composite in principal symmetry directions of the material. The constitutive equations for the laminated composite result from the combination of lamina constitutive equations that also result from the combination of fibers and matrix. It is assumed that each one of the components are orthotropic and elastoplastic. Basic assumptions of the proposed model and the resulting equations are first presented in the paper. The numerical algorithm developed for the implementation in a three-dimensional (3D) finite element nonlinear program is also described. The paper is completed with application examples and comparison with experimental results. The comparison shows the capacity of the proposed model for the simulation of stiffness and strength of different composite laminates.
[DOI: 10.1115/1.2200654]

1 Introduction

In recent years, considerable attention has been focused on the modeling of composite materials as conventional materials are continuously being replaced by a variety of composite materials. Several approaches have been developed but there is still a strong need of predicting models that can be used for stiffness and strength assessment of this type of materials in actual situations without the need of many empirical constants.

Constitutive models for fiber reinforced composite laminates can be classified according to the scale in which they are defined [1]. In macro-models the composite material is represented as a unique material with average properties. This type of approach generally results insufficient to describe the overall behavior inelastic and failure behavior of the laminate. In meso-models the composite is assumed to be formed by unidirectional laminas for which macroscopic equations are derived. The constitutive properties of individual laminas are obtained from experimental tests. In contrast, micro-models use the constitutive equations of the elemental constituents: Matrix, fibers, interfaces, etc. This approach has the advantage of allowing the identification of the failure mode but requires accurate experimental data for the individual components, which is not generally available. An alternate approach is the use of multi-scale models [2].

Many micromechanical models have been developed for fiber reinforced composites but most of them have considerable limitations. Theories are generally too complicated or, when they are simple, they are only able to reproduce a few aspects of the behavior in fiber directions or they are only valid for composites in which stiffness and strength of the fibers are significantly greater than those of the matrix [3].

Contributed by the Applied Mechanics Division of ASME for publication in the JOURNAL OF APPLIED MECHANICS. Manuscript received May 21, 2005; final manuscript received March 27, 2006. Review conducted by G. C. Buscaglia. Discussion on the paper should be addressed to the Editor, prof. Robert M. McMeeking, Journal of Applied Mechanics, Department of Mechanical and Environmental Engineering, University of California—Santa Barbara, Santa Barbara, CA 93106-5070, and will be accepted until four months after final publication of the paper itself in the ASME JOURNAL OF APPLIED MECHANICS.

Hinton and Soden recently organized a "failure exercise" to compare the predictive capabilities of a number of the most important strength theories for laminated composites in current usage [4–8]. The results of that exercise [9–12] were used for the assessment of the accuracy of current theoretical methods of failure prediction in composite laminates. According to Soden et al. [12], the most reliable theories for the designer are the theories of Zinoviev et al. [13,14], Bogetti [15], Tsai [16,17], Puck [18,19], and Cuntze [20].

None of these five theories is based on a micromechanics analysis. Huang [3] developed a micromechanical model to estimate the strength of unidirectional fibre reinforced composites. Fibers and matrix are considered to be elastoplastic with very simple linear hardening laws defined for each direction. The stress in each component is expressed in terms of the global stress using a bridging matrix. Nevertheless, the accuracy of the strength predictions for this theory is moderate [12].

A numerical model for general composite materials, appropriate for the mechanical analysis of fiber reinforced composite laminates, is presented in this paper. The model is based on an analysis at component materials level that allows obtaining, at a first stage, the behavior of the lamina from the mechanical properties of matrix and fibers, their volume ratio and their orientation. Then, the behavior of the laminate can be obtained composing laminas with different fiber orientations. The model is completely general and can be used for other types of composites.

The model is based on very simple kinematical and equilibrium assumptions that, properly handled, lead to composite constitutive equation and the strain and stress tensors in all the components. In this way, elastic properties of the laminate can be obtained. Nonlinear behavior and the progressive failure can be analyzed and failure envelopes can be defined.

The novelty of the model presented is the development of a formalism that allows dealing with equal stress or equal strain in correspondence with each stress (or strain) component in a systematic way and that is applicable to various kinds of composite topologies. The model can be interpreted as a generalization of Reuss' and Voight's theories that can also deal with general orthotropic elastoplastic models for each one of the constituents mate-

rials. Moreover, resulting equations are very simple and resemble those of mixing theory allowing a similar numerical treatment.

2 Proposed Model

2.1 Introduction. This model assumes that the composite can be subsequently decomposed in sub-composites to arrive to composites with simple structure for which simple kinematical and equilibrium hypothesis relating stress and strain of the components can be stated. Basically, for this composite with simple structure it should be clear which strain components are common to all components (parallel behavior) and which stress components are common to all components (series behavior).

Successive decompositions are generally required in order to state these assumptions. Particularly, in the case of reinforced fiber laminated composites, the laminate should be separated in laminas and each lamina should be analyzed first. It will be noted later in application examples that even the precise analysis of one individual unidirectional lamina should require more than one decomposition.

2.2 Constitutive Model for the Components. It is well known that fibers present a strong anisotropic behavior, generally assumed as transversely isotropic, characterized not only by the elastic orthotropy like in the case of carbon fibers but also by the marked difference of strength in principal directions. Another important property of fibers is their slightly lower strength in compression than in tension [21].

APC: #1

In general, epoxy resins have lower tension than compression strength like brittle materials. In the case of polymeric matrix the material itself can be supposed to be isotropic. Nevertheless, as the fiber/matrix interface is not explicitly modeled, the constitutive model of the matrix is modified including the interface constitutive model [22,23]. Orthotropic elastoplastic or damage interface models can be used to simulate fiber debonding or delamination. As a result, the constitutive model of the matrix including interface exhibits a tension strength much lower in perpendicular direction to fiber than in longitudinal direction.

Taking into account the above considerations, each one of the basic components is supposed to have a general orthotropic elastoplastic behavior covering the case of fibers, matrix, and interface included in matrix.

The orthotropic model used is based on the assumption that there are two spaces [24–26]: (a) A real anisotropic space and (b) a fictitious isotropic space. The problem is solved in the fictitious isotropic space allowing the use of elastoplastic models originally developed for isotropic materials. The isotropic elastoplastic model used in this paper includes energy-based criteria to make it suitable for brittle materials [27].

Stress tensors in both spaces are related by a tensor transformation that can be written as,

$$\tau = \boldsymbol{A}(\sigma, \kappa^p):\sigma \tag{1}$$

where τ and σ are the stress tensors in spaces (a) and (b), respectively, and $\boldsymbol{A}$ is a fourth-order transformation tensor that contains the information about strength anisotropy depending on material symmetry. In the most general case, this tensor varies with the stress state and the evolution of the inelastic process represented by the isotropic plastic hardening variable κ^p [26]. In this paper, all the components materials are assumed initially orthotropic with 3 axes of material symmetry. There are different alternatives to define tensor $\boldsymbol{A}$ for this case [25,26,28–30]. The simplest way is a diagonal fourth-order tensor [27],

$$A_{ijkl} = \delta_{im}\delta_{jn}\delta_{km}\delta_{\ln}\bar{\tau}/\bar{\sigma}_{mn} \tag{2}$$

where $\bar{\tau}$ is the strength in the fictitious isotropic space and $\bar{\sigma}_{mn}$ is the actual strength in the direction m in the plane with normal n. A better approach has been proposed by Oller et al. [30].

The model is thermodynamically consistent and it is based on the assumption of uncoupled elasticity. The free energy density can be supposed to be formed by two independent parts: An elastic part Ψ^e and a plastic part Ψ^p,

$$\Psi = \Psi^e + \Psi^p \quad \Psi^e = \tfrac{1}{2}\varepsilon^e:\boldsymbol{C}:\varepsilon^e \tag{3}$$

where $\boldsymbol{C}$ is the stiffness tensor and ε^e is the elastic strain tensor.

The secant constitutive equation can be deduced from the free energy density as follows,

$$\sigma = \partial\Psi^e/\partial\varepsilon^e = \boldsymbol{C}:\varepsilon^e = \boldsymbol{C}:(\varepsilon - \varepsilon^p) \tag{4}$$

where ε is the strain tensor and ε^p is the plastic strain tensor.

The plastic threshold is defined through a yielding function,

$$F(\sigma;\alpha) = \bar{F}(\tau;\bar{\alpha}) = 0 \tag{5}$$

where F and $\bar{F}$ represent the yielding function in the real anisotropic space and the fictitious isotropic space, respectively; α and $\bar{\alpha}$ are internal variables in correspondence with both spaces.

The transformation defined by Eq. (1) allows the use of yielding functions $\bar{F}$ defined for isotropic materials in the fictitious isotropic space. It should be noted that this space is isotropic with respect to yielding thresholds and strength but not necessarily with respect to other properties like elastic stiffness.

Evolution of plastic strain in real space is defined with the well-known flow rule,

$$\dot{\varepsilon}^p = \dot{\lambda}(\partial G/\partial\sigma) \tag{6}$$

where G is the plastic potential function defined in the real stress space. Instead of working with this function that should be anisotropic, function $\bar{G}$ defined in the fictitious isotropic space could be used.

$$G(\sigma,\alpha) = \bar{G}(\tau,\bar{\alpha}) \tag{7}$$

Equation (5) can be then rewritten as,

$$\dot{\varepsilon}^p = \dot{\lambda}(\partial\bar{G}/\partial\sigma) = \dot{\lambda}(\partial\bar{G}/\partial\tau):(\partial\tau/\partial\sigma) = \dot{\lambda}(\partial\bar{G}/\partial\tau):\boldsymbol{H} = \dot{\lambda}\bar{\boldsymbol{h}}$$

$$with \quad \boldsymbol{H} = \partial\tau/\partial\sigma \quad and\ \bar{\boldsymbol{h}} = (\partial\bar{G}/\partial\tau):\boldsymbol{H} \tag{8}$$

where $\boldsymbol{H}$ is a fourth-rank tensor and $\bar{\boldsymbol{h}}$ is a second-rank tensor and represents the plastic flux in the real orthotropic space.

2.3 Kinematical and Equilibrium Assumptions. In a composite with a simple structure there are three orthogonal directions referred to which some strain components are common to all constituents (parallel behavior) and the rest of the components are associated to equal stress in all constituents (series behavior). A parallel behavior in correspondence with one component means that all the composite constituents have the same value for this strain component. A series behavior in correspondence with one component means that all the composite constituents have the same value for this stress component. As an example, consider a composite with the representative structure shown in Fig. 1(*a*). It is clear that σ_{11} is common for both components (series behavior) while ε_{22} and ε_{33} are common for both components (series behavior). For a more complex structure like that represented in Fig.

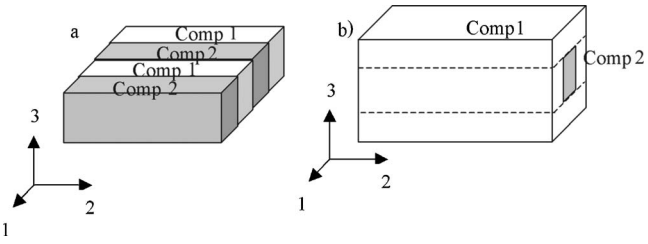

Fig. 1 Schematic representation of composite structure. (*a*) Simple structure, (*b*) More complex structure.

1(*b*), this type of conclusions can not be stated a priori, but the composite can be considered to be formed by the sub-composites with simple structure indicated with dashed lines.

Based on this analysis, stress and strain components could be rearranged. All the stress and strain components that are common to all components are grouped in tensor ε^*, while all the stress and strain components that will be obtained as a superposition of the contribution of all constituents are grouped in tensor σ^*.

In order to express this rearrangement the following fourth order tensors are defined,

$$\alpha^{\sigma}_{ijkl} = \delta_{ir}\delta_{js}\delta_{kr}\delta_{ls}H(p_{rs})$$
$$\alpha^{\varepsilon}_{ijkl} = \delta_{ik}\delta_{jl} - \alpha^{\sigma}_{ijkl}$$
$$with\ p_{rs} = \begin{cases} 1 \text{ if the } rs \text{ component works in parallel} \\ 0 \text{ if the } rs \text{ component works in series} \end{cases} \tag{9}$$

H: Threshold function.

According to Eq. (9), the product $\alpha^{\sigma}:\sigma$ preserves the stress components that are assumed to have a parallel behavior and make the other components zero.

Stress and strain components are rearranged as follows,

$$\begin{aligned} \sigma^* &= \alpha^{\sigma}:\sigma + \alpha^{\varepsilon}:\varepsilon \\ \varepsilon^* &= \alpha^{\varepsilon}:\sigma + \alpha^{\sigma}:\varepsilon \end{aligned} \quad \text{and} \quad \begin{aligned} \sigma &= \alpha^{\sigma}:\sigma^* + \alpha^{\varepsilon}:\varepsilon^* \\ \varepsilon &= \alpha^{\varepsilon}:\sigma^* + \alpha^{\sigma}:\varepsilon^* \end{aligned} \tag{10}$$

where σ^* contains stress components in correspondence with directions of parallel behavior and strain components in correspondence with directions of series behavior. Tensor ε^* contains strain components in correspondence with directions of parallel behavior and stress components in correspondence with directions of series behavior

2.4 Alternative Way of Writing Constitutive Equations of the Components. An alternative way of writing constitutive equations of the components that makes the development of the constitutive equation of the composites easier is proposed in this section.

Combining Eqs. (3) and (10), the following secant constitutive relation can be obtained,

$$\sigma^* = C^*:\varepsilon^* - \sigma^{p^*} \tag{11}$$

where,

$$C^* = (\alpha^{\sigma}:C + \alpha^{\varepsilon}):(\alpha^{\varepsilon}:C + \alpha^{\sigma})^{-1} \tag{12}$$

$$\sigma^{p^*} = (C^*:\alpha^{\sigma} - \alpha^{\varepsilon}):\varepsilon^p \tag{13}$$

2.5 Composite Constitutive Equation. First, the case of a composite with simple structure where principal directions and tensors α^{σ} and α^{ε} are coincident for all the constituents is analyzed. In such composite, the following condition is verified,

$$\varepsilon^*_c = \varepsilon^* \tag{14}$$

where c indicates an arbitrary component material.

Assuming that the plastic strain of the composite in the directions in which the material works in series can be obtained as the sum of the plastics strains of the components multiplied by their respective volume fractions, the following secant equation is obtained,

$$\sigma^* = \boldsymbol{C}^*:\varepsilon^* - \sigma^{p^*} \tag{15}$$

where,

$$\boldsymbol{C}^* = \sum k_c \boldsymbol{C}^*_c \quad \sigma^{p^*} = \sum k_c(\boldsymbol{C}^*_c:\alpha^{\sigma} - \alpha^{\varepsilon}):\varepsilon^p_c \tag{16}$$

And $\boldsymbol{k}_c$ represents the volume fraction of a generic constituent material.

Equation (15) can be rearranged with the aid of Eqs. (10) to give,

$$\sigma = \boldsymbol{C}:\varepsilon - \sigma^p \tag{17}$$

where,

$$\boldsymbol{C} = (\alpha^{\sigma}:\boldsymbol{C}^* + \alpha^{\varepsilon}):(\alpha^{\varepsilon}:\boldsymbol{C}^* + \alpha^{\sigma})^{-1}$$

$$\sigma^p = -\boldsymbol{C}:\alpha^{\varepsilon}:\sigma^{p^*} + \alpha^{\sigma}:\sigma^{p^*} = (\alpha^{\sigma} - \boldsymbol{C}:\alpha^{\varepsilon}):\sigma^{p^*} \tag{18}$$

Numerical implementation in a finite element program requires the evaluation of the strain tensor for each one of the components from the composite strains. In this way, once the strains are known, constitutive equations can be independently integrated for each constituent and information at the constituents material level (fiber and matrix) level can be recorded through the corresponding internal variables.

Starting from condition (14) and Eqs. (10) and (17), the following relation can be written,

$$\varepsilon_c = \phi_c:\varepsilon + \tilde{\varepsilon}^p_c \tag{19}$$

where,

$$\phi_c = (\alpha^{\varepsilon}:\boldsymbol{C}^*_c + \alpha^{\sigma}):(\alpha^{\varepsilon}:\boldsymbol{C}^* + \alpha^{\sigma})^{-1}$$

$$\tilde{\varepsilon}^p_c = \phi_c:\alpha^{\varepsilon}:\sigma^{*P} - \alpha^{\varepsilon}:\sigma^{*P}_c \tag{20}$$

The elastoplastic tangent tensor can be obtained from the derivation of Eq. (16)

$$\dot{\sigma} = \boldsymbol{C}:\dot{\varepsilon} - \dot{\sigma}^p = \boldsymbol{C}^T:\dot{\varepsilon} \tag{21}$$

and results,

$$\boldsymbol{C}^T = \boldsymbol{C} - (\alpha^{\sigma} - \boldsymbol{C}:\alpha^{\varepsilon}):\sum k_c(\boldsymbol{C}^*_c:\alpha^{\sigma} - \alpha^{\varepsilon}):(\boldsymbol{I} - \boldsymbol{C}^{-1}_c:\boldsymbol{C}^T_c):\phi_c \tag{22}$$

where $\boldsymbol{C}^T_c$ is the elastoplastic tangent tensor of component c.

All the preceding equations are only valid in the composite local system of reference coincident with its principal symmetry directions. For an arbitrary reference system, all tensors must be rotated.

2.6 More Complex Composites. The constitutive equations for a laminated composite or for a composite material with a more complex structure, where the tensors α^{σ} and α^{ε} are not the same for all components, can be obtained in different steps. The composite must be decomposed in more simple sub-composites for which the correspondent constitutive equations can be obtained as described above. Then, the constitutive equation of the composite, can be written with a similar approach, composing the constitutive equations already found for the sub-components. For example, the constitutive equation of a laminate composed by n fiber reinforced laminas with different properties, in principal directions of the laminate would look like Eqs. (17) and (18) where the tensors α^{σ} and α^{ε} are related to the laminate structure and the tensors C^* and σ^{p*} are calculated as follows,

$$\boldsymbol{C}^* = \sum_{c=1}^{n} k_c \boldsymbol{C}^*_c \tag{23}$$

$$\boldsymbol{C}^*_c = (\alpha^{\sigma}:\boldsymbol{R}_c \,.\, \boldsymbol{R}_c \,.\, \boldsymbol{C}_c \,.\, \boldsymbol{R}^t_c \,.\, \boldsymbol{R}^t_c + \alpha^{\varepsilon}):(\alpha^{\varepsilon}:\boldsymbol{R}_c \,.\, \boldsymbol{R}_c \,.\, \boldsymbol{C}_c \,.\, \boldsymbol{R}^t_c \,.\, \boldsymbol{R}^t_c + \alpha^{\sigma})^{-1} \tag{24}$$

$$\boldsymbol{C}_c = \left(\alpha^{\sigma}_c:\sum_{i=1}^{2} k_{ci}\boldsymbol{C}^*_{ci} + \alpha^{\varepsilon}_c\right):\left(\alpha^{\varepsilon}_c:\sum_{i=1}^{2} k_{ci}\boldsymbol{C}^*_{ci} + \alpha^{\sigma}_c\right)^{-1} \tag{25}$$

$$\boldsymbol{C}^*_{ci} = (\alpha^{\sigma}_c:\boldsymbol{C}_{ci} + \alpha^{\varepsilon}_c):(\alpha^{\varepsilon}_c:\boldsymbol{C}_{ci} + \alpha^{\sigma}_c)^{-1} \tag{26}$$

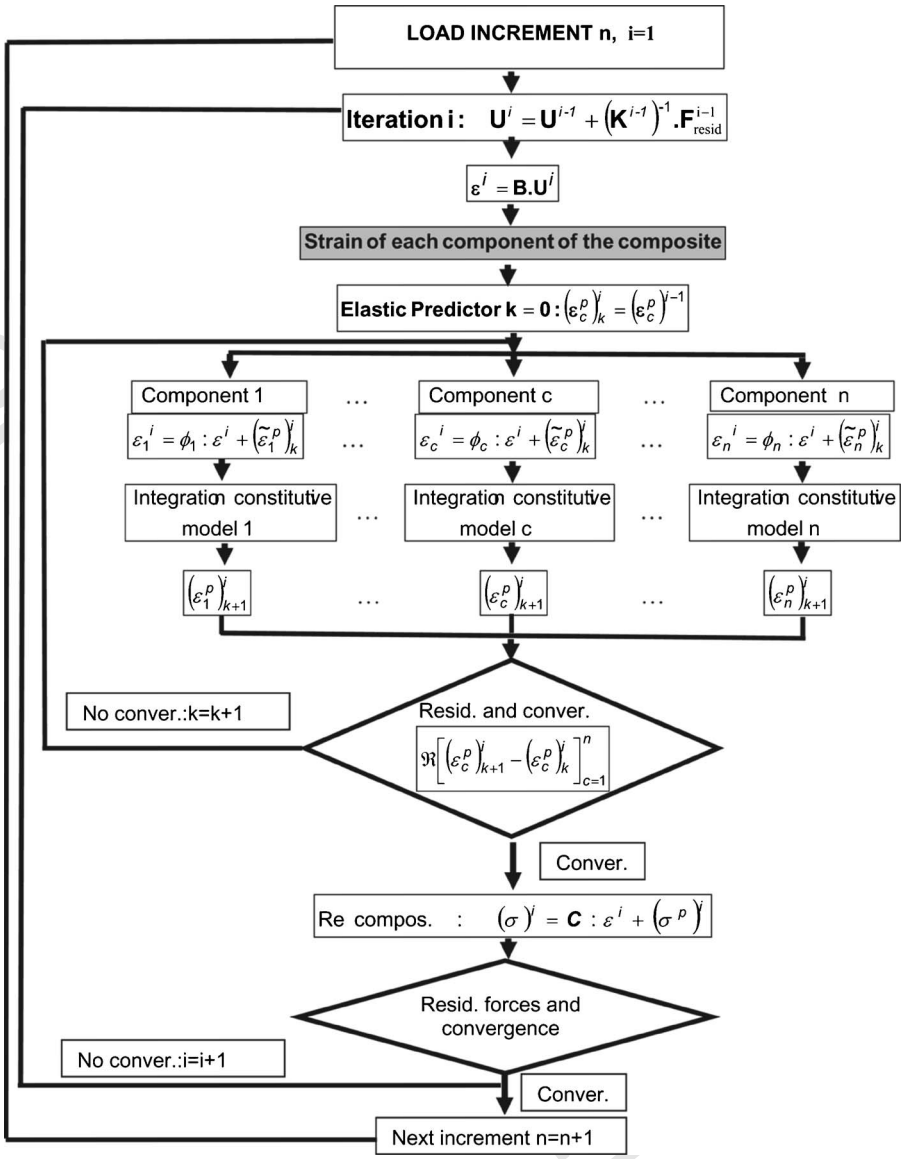

Fig. 2 Numerical scheme for the solution of a nonlinear problem

$$\sigma^{p^*} = \sum_{c=1}^{n} k_c(\boldsymbol{C}_c^*:\alpha^\sigma - \alpha^\varepsilon):\boldsymbol{R}^{t-1} \,.\, \varepsilon_c^p \,.\, \boldsymbol{R}^{-1} \tag{27}$$

$$\varepsilon_c^p = \boldsymbol{C}_c^{-1}:\sigma_c^p = \boldsymbol{C}_c^{-1}:(\alpha_c^\sigma - \boldsymbol{C}_c:\alpha_c^\varepsilon):\sigma_c^{p^*} \tag{28}$$

$$\sigma_c^{p^*} = \sum_{i=1}^{2} k_{ci}(\boldsymbol{C}_{ci}^*:\alpha_c^\sigma - \alpha_c^\varepsilon):\varepsilon_{ci}^p \tag{29}$$

where $\boldsymbol{R}_c$ is the rotation matrix from lamina c principal coordinates to laminate principal coordinates, the tensors α_c^σ and α_c^ε are related to the lamina c, k_c is the volume fraction of lamina c, k_{ci} is the volume fraction of the component i in lamina c, $\boldsymbol{C}_{\mathrm{ci}}$ is the secant stiffness tensor of the same component in lamina local coordinates, and ε_{ci}^p is the permanent strains tensor of component i in lamina c in local lamina coordinates.

Delamination can be included in the model presented using an approach similar to that used for fiber debonding [22,23]. A term due to differential strains among laminas, depending on interlaminar stress, should be added in Eq. (27).

3 Numerical Implementation

The model presented can be implemented in a nonlinear finite element program using the iterative scheme presented in Fig. 2. A composite with simple structure strains in each component can be evaluated with Eq. (19) if plastic strains are known. In case of a more complex composite, this scheme must be used to decompose the composite in sub-composites and again inside each sub-composite to arrive to each one of the constituents.

In any case, plastic strains of all components are required for the evaluation of the strains in each component. As a result, the problem cannot be explicitly solved and, for example, an iterative scheme must be used. The algorithm schematized in Fig. 2 is based on a predictor-corrector iterative procedure using the norm of plastic strains as convergence measure.

Once the strains of each one of the constituents have been obtained, the correspondent constitutive equations can be integrated using well-known procedures like Euler backward or return mapping algorithms.

Failure envelopes can be obtained with a finite element program loading an element with different stress combinations up to

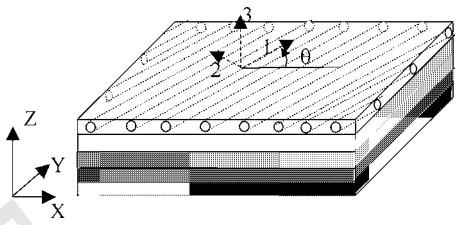

Fig. 3 Fiber reinforced laminated composite

failure. Each stress ratio gives a point of the failure envelope. Alternatively, failure envelopes for composites with simple structure can be analytically obtained writing the yielding criteria of each component, Eq. (5), in terms of the composite stress tensor. In this type of composites it is simple to analyze which is the failure mechanism without any nonlinear calculation.

4 Application Examples

4.1 Introduction. A scheme of a laminated is shown in Fig. 3 where the principal directions used as references are also indicated. In the case of unidirectional laminas, the components can be supposed to work in parallel in fiber directions 1 and 3 (the same strain for all components) and in series in direction 2 (the same stress for all components). The way in which shear is resisted is not so clear and depends, among other factors, on the shape of the fibers transverse section. In general, a more complex combination is required to accurately reproduce shear transfer inside the composite.

In the case of the laminate, principal directions X and Y are contained in the laminate plane and direction Z is orthogonal to that plane. Each lamina can exhibit a different fiber orientation that is defined through the angle θ that forms lamina principal direction 1 with principal direction X of the laminate (see Fig. 4). It can be assumed that laminas work in parallel in the laminate plane and in series in the orthogonal direction.

In general, structures are not designed with all the fibers aligned in a unique direction if the structure is expected to be exposed to stresses in the orthogonal direction. However, unidirectional laminas constitute the basic elements of the laminate and, inside it, they can be exposed to stresses normal to the fiber direction and shear stresses. It is important then to know first if the models are able to reproduce the behavior of individual laminas.

4.2 Elastic Properties of an Unidirectional Lamina. Elastic properties of an epoxy lamina with carbon fibers are studied in this section. Elastic properties of each one of the constituents are the following,

$$E_{1f} = 232 \text{ GPa}; \quad E_{2f} = 15 \text{ GPa}; \quad \nu_{12f} = 0.279;$$

$$\nu_{23f} = 0.49; \quad G_{12f} = 30.2 \text{ GPa};$$

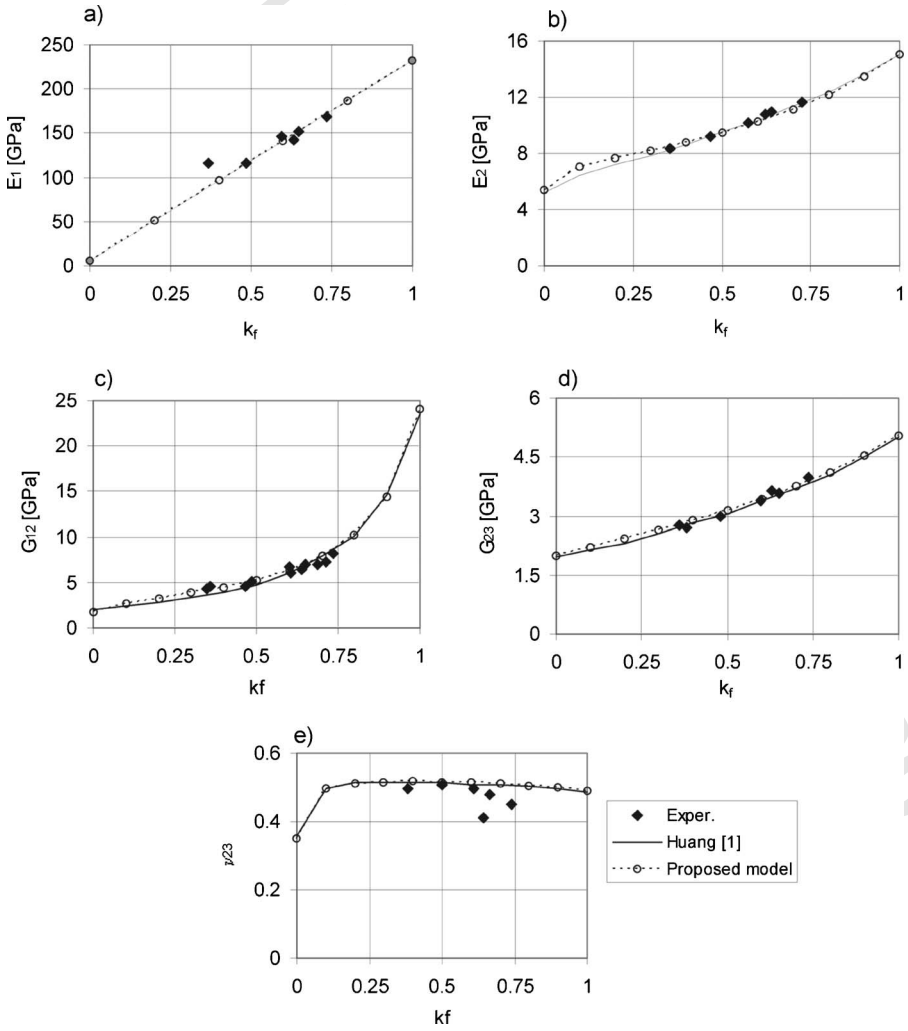

Fig. 4 Elastic properties of the lamina as a function of fiber fraction. (*a*) E_1, (*b*) E_2, (*c*) G_{12}, (*d*) G_{23}, (*e*) ν_{23}.

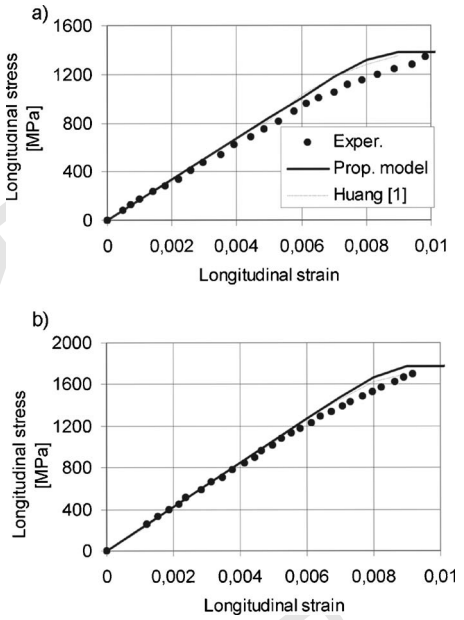

Fig. 5 Stress-strain behavior in the fiber direction. (*a*) $k_f = 0.20$, (*b*) $k_f = 0.35$.

$$E_m = 5.35 \text{ GPa}; \quad \nu_m = 0.22$$

The variations of longitudinal and transverse Young modulus E_1 and E_2, longitudinal and transverse shear modulus G_{12} and G_{23} and Poisson ratio ν_{23} as a function of fiber volume fraction k_f are shown in Fig. 4. The experimental results obtained by Kriz and Stinchcomb [31] and analytical results by Huang [3] are also plotted on Fig. 4. In all cases, a good agreement between the proposed model and experimental results is obtained. It should be noted that in this case where fibers are supposed to be orthotropic, elastic modulus E_2 can be accurately estimated with the assumption of series behavior in direction 2. In contrast, for transverse elastic modulus G_{12} and G_{23} a series/parallel combination gives better results.

4.3 Strength and Nonlinear Behavior of an Unidirectional Lamina. The nonlinear behavior of a lamina composed of unidirectional SiC brittle fibers and a Titanium matrix is analyzed in this section. The mechanical properties of the constituent materials are the following,

$$E_f = 400 \text{ GPa}; \quad \nu_f = 0.25; \quad Y_f^u = 1000 \text{ MPa};$$

$$E_m = 106 \text{ GPa}; \quad E_m^T = 7.6 \text{ GPa}; \quad Y_m^y = 850 \text{ MPa};$$

$$Y_m^u = 1000 \text{ MPa}; \quad \nu_m = 0.33$$

where Y_m^y and Y_m^u are the matrix yield stress and ultimate strength, respectively, and Y_f^u is the fibers ultimate strength.

The stress-strain behavior in the direction of the fibers for two different fiber volume fractions is presented in Fig. 5. Numerical results are compared with experimental ones obtained by Gundel [32] and analytical ones given by [3]. A good agreement with analytical and experimental results is obtained.

4.4 Composite Laminates. Material data and the different types of analysis presented in this section correspond to the failure exercise previously mentioned [5,7]. All the laminates studied are formed by laminas composed of a soft matrix with continuous unidirectional fibers. The mechanical properties of four types of epoxy resins and four types of glass and carbon fibers are presented in Tables 1 and 2, respectively. The determination of the mechanical properties is not always straightforward. As a consequence, variability and inaccuracy are expected to be found.

Table 1 Matrix mechanical properties [3]

Type of Matrix	3501-6 epoxy	BSL914C epoxy	LY556/HT907/DY063 epoxy	MY750/HY917/DY063 epoxy
Young modulus, E_m (GPa)	4.2	4.0	3.35	3.35
Shear modulus, G_m (GPa)	1.567	1.481	1.24	1.24
Poisson ratio, ν_m	0.34	0.35	0.35	0.35
Tension strength, Y_{mt} (MPa)	69	75	80	80
Compres. strength, Y_{mc} (MPa)	250	150	120	120
Shear strength, S_m (MPa)	50	70	⋯	⋯
Ultimate tension strain., ε_{mt} (%)	1.7	4	5	5

Almost all experimental results used were derived from tests on tube specimens. Numerical results were all obtained for a 100 mm × 100 mm model with the lamina or laminate thickness and a three-dimensional analysis was performed. The use of these models is justified by the fact that in tube specimens a global plane stress state for the lamina or the laminate is obtained.

4.4.1 Unidirectional Laminas. Before analyzing the behavior of the laminate it is interesting to analyze the behavior of unidirectional laminas under biaxial tension tests to obtain the corresponding failure envelopes. In all cases, a Mohr Coulomb failure criterion was used for the matrix while a Drucker Prager criterion was used for the fibers failure.

Figure 6 shows the comparison of the failure envelope obtained using the proposed model with experimental results [7] and with other numerical models [12] for an unidirectional glass fiber reinforced lamina (E-Glass/LY556/HT907/DY063), with a fiber volume fraction k_f=0.62, under shear stresses and normal stresses orthogonal to fiber direction. Experimental results correspond to tubes of 60 mm internal diameter and 2 mm thick. It can be observed that the model closely reproduces the experimental failure envelope. For this particular example, the failure is always produced by the matrix failure.

Figure 7 shows the comparison of failures stresses obtained using the model proposed and other numerical models [11] with experimental ones [7] for an unidirectional carbon fiber reinforced lamina (T300/BSL914C epoxy), with a fiber volume fraction k_f =0.60, under shear stresses and normal stresses in the direction of the fibers. Experimental results were obtained from tubes tested under combined axial tension or compression and torsion. The tubes were 32 mm diameter and 1.9–2.3 mm thick. In this ex-

Table 2 Fibers mechanical properties [3]

Type of fiber	AS4	T300	E-Glass 21×43 Gevetex	Silenka E-Glass 1200 tex
Long. Young modulus, E_{f1} (GPa)	225	230	80	74
Transv. Young modulus, E_{f2} (GPa)	15	15	80	74
Long. shear. modulus, G_{f12} (GPa)	15	15	33.33	30.8
Poisson ratio ν_{f12}	0.2	0.2	0.2	0.2
Transv. shear modulus., G_{f23} (GPa)	7	7	33.33	30.8
Long. tensile strength, X_{fl} (MPa)	3350	2500	2150	2150
Long. compres. strength, X_{fc} (MPa)	2500	2000	1450	1450
Ultimate tensile strain, ε_{f1T} (%)	1.488	1.086	2.687	2.905
Ultimate compres. strain, ε_{f1c} (%)	1.111	0.869	1.813	1.959

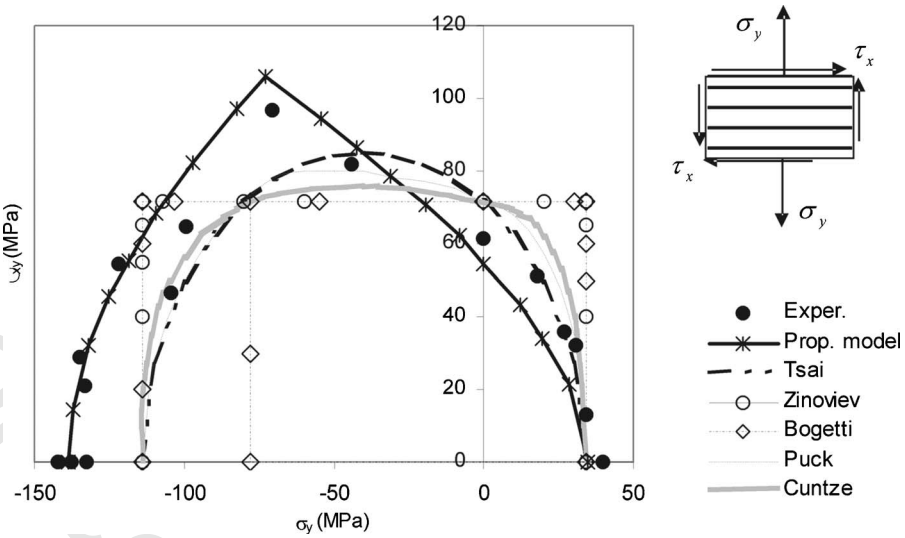

Fig. 6 Failure envelope for a unidirectional lamina (E-Glass/LY556/HT907/DY063)

ample, failure is generated by the failure of the fibers for moderated shear stresses or by the matrix failure for greater shear stresses. It could be seen that the model approximately reproduces the lamina failure envelope but does not result conservative in the zone corresponding to compression in fiber direction because it is not able to capture buckling and associated failure.

Figure 8 shows the comparison of the failure envelope obtained using the model and other numerical models [12] with experimental results [7] for an unidirectional glass fiber reinforced lamina (Silenka E-Glass 1200 tex MY750/HY917/DY063 epoxy),l with a fiber volume fraction k_f=0.60 under normal stresses in the direction of the fibers and in the orthogonal one. Most of the experimental results were obtained from testing nearly circumferentially wound tubes under combined internal pressure and axial load. The specimens were 100 mm inner diameter, 300 mm long and approximately 0.95 mm or 1.2 mm thick. In this case, the failure is produced by the fibers failure when the stress in fiber direction is prevalent or by the matrix failure in the directional perpendicular to the fibers.

4.4.2 Laminates

4.4.2.1 $(90\ \text{deg}/\pm 30\ \text{deg})_s$ *Laminate (E-Glass/LY556/HT907 /DY063).* The structure of this laminate is indicated in Fig. 9. Soden et al. [5] use a different nomenclature but refer to a $(90/\pm 30\ \text{deg})_s$ laminate. The angle indicated corresponds to the angle of the fibers to axe *X* that is coincident with the axe of the tubes experimentally tested. The total thickness of the laminate is 2 mm, while h_1=0.172 mm and h_2=0.414 mm. As a consequence, laminas at ±30 deg represent 82.8% of the total thickness and laminas at 90 deg represent the remaining 17.2%. The laminate is not isotropic and, therefore, different types of failure under biaxial stresses can take place, not only those due to fibers failure. The fiber volume fraction of each lamina is k_f=0.62. Experimental results were obtained from 60 mm inside diameter and 2 mm thick tubes tested under combined pressure and axial load and combined torsion and axial load.

Figures 9(*a*) and 9(*b*) show the failure envelopes obtained with the model for this laminate under biaxial stresses and their com-

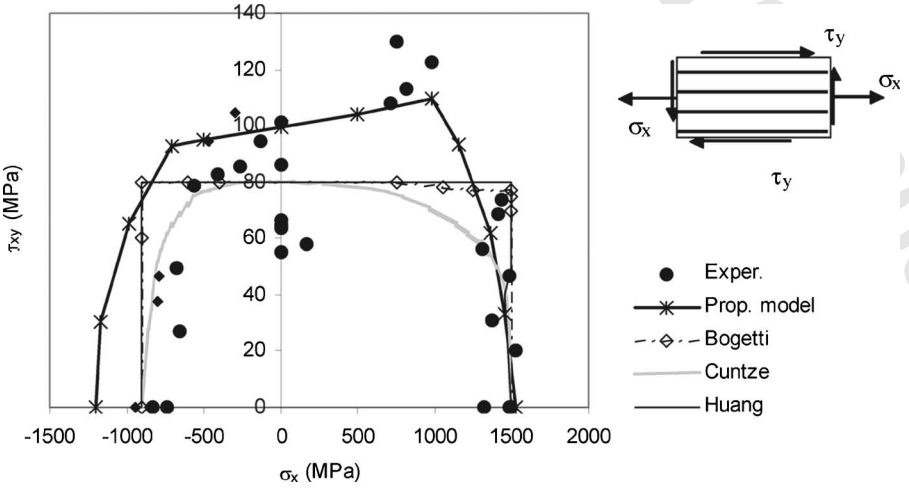

Fig. 7 Failure envelope for a unidirectional lamina (T300/BSL914C epoxy)

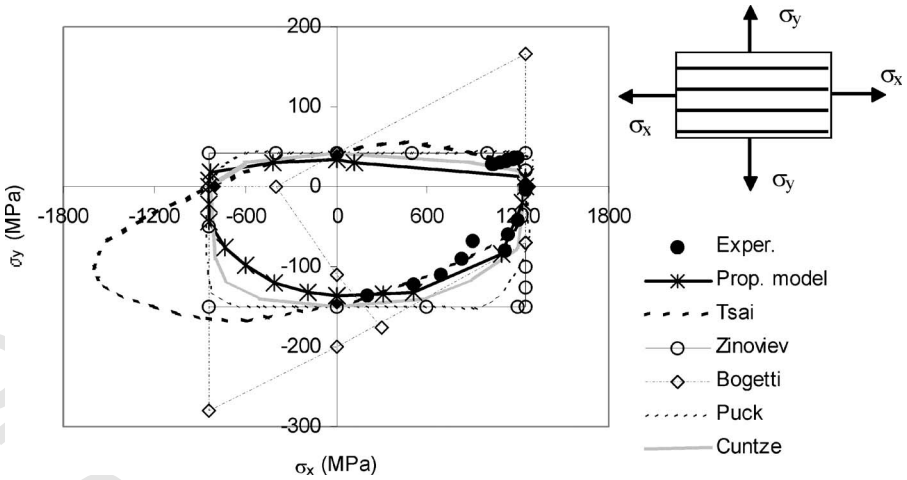

Fig. 8 Failure envelope for a unidirectional lamina (Silenka E-Glass 1200 tex MY750/ HY917/DY063 epoxy)

parison with experimental results [7] and other theories [11]. Figure 9(*a*) corresponds to different combinations of normal stresses in the plane. Failure is due to matrix failure in the compression-compression zone and it is caused by fiber failure for most of the other stress combinations. Figure 9(*b*) represents a combination of normal and shear stresses. Composite failure is due to matrix failure in compression zone and it is mostly due to fiber failure in pure shear and tension zones. In general, the model reproduces experimental results but leads to nonconservative results under biaxial compression stress states.

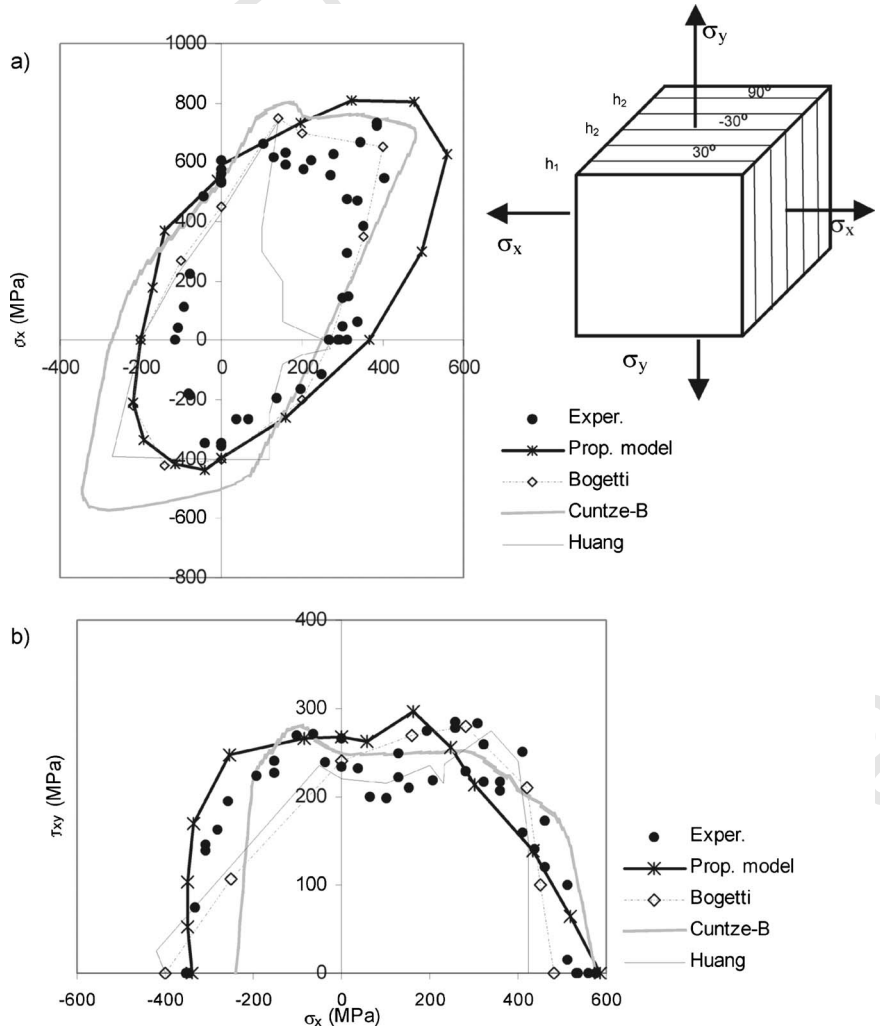

Fig. 9 Failure envelope for a (90 deg/ ±30 deg)$_s$ laminate (E-Glass/LY556/HT907/DY063). (*a*) $_x\sigma$ versus σ_y; (*b*) τ_{xy} versus σ_x.

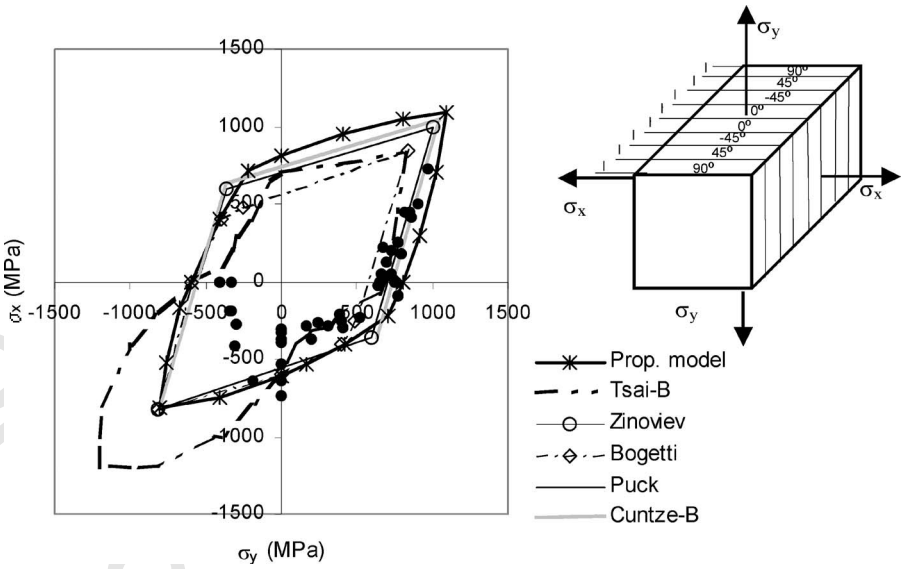

Fig. 10 Failure envelope for (90 deg/±45 deg/0 deg)$_s$ laminate (AS4/3501-6)

4.4.2.2 (90 deg/±45 deg/0 deg)$_s$ *Laminate AS4/3501-6*. The structure of this quasi isotropic laminate is shown in Fig. 10. The total thickness of the laminate is 1.1 mm and all the laminas have the same thickness. The fiber volume fraction of each lamina is k_f=0.60. The tests were carried out by subjecting 96 mm inside diameter tubular specimens to pressure and axial loads.

Figure 10 shows the failure envelope obtained with the model and its comparison with experimental results [7] and other theories [12] for biaxial stress states. In general, the tests have shown failure by fibers fracture being the failure controlled by fibers strength. Experimental results in the compression-compression quadrant represent structural failure produced by buckling of the laminate and not by crushing of the material. Numerical results confirm that composite failure is due to fiber failure and dependent on fibers compressive and tensile strength. In general, the model results are close to experimental ones except those in the compression-compression zone where the model is not able to reproduce buckling failure.

4.4.2.3 (±55 deg)$_s$ *Laminate (Silenka E-Glass 1200 tex MY750/HY917/DY063 epoxy)*. The structure of this laminate is shown in Fig. 11. The total thickness of the laminate is 1 mm and all the laminas have the same thickness. The fiber volume fraction of each lamina is k_f=0.60. Experimental results were obtained from tubes with 100 mm inner diameter and 1 mm thick.

Figure 11 also shows the failure envelope obtained with the model and its comparison with experimental results [7] and other theories [12]. Numerical results show that failure is mostly due to fiber failure, except for the zone where the failure envelope narrows that corresponds to matrix tensile failure. A good agreement between numerical and experimental results is achieved.

5 Conclusions

A general model for composite materials that starts from a simple idealization of the behavior at individual constituents level has been presented in this paper. The model gives the behavior of

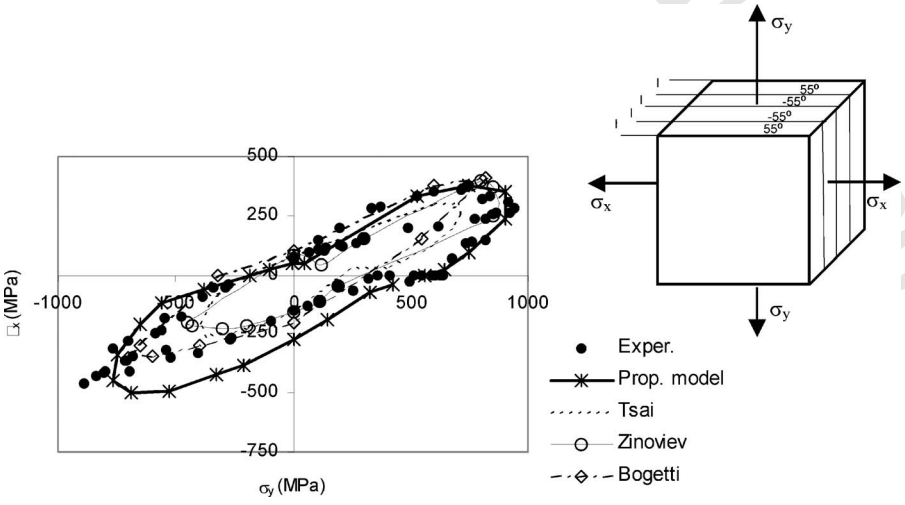

Fig. 11 Failure envelope for (±55 deg)$_s$ laminate (Silenka E-Glass 1200 tex MY750/HY917/DY063 epoxy)

a composite material from the constitutive models of the components, their location in the composite and volume fraction. Due to its assumptions the model is especially appropriate for the treatment of fiber reinforced composite laminates. It allows the anisotropy and nonlinear behavior of the materials to be considered.

The resulting model describes the behavior and the failure of the composite taking into account what is happening in each component and it is able to identify the failure mode of the composite produced by the failure of one or more components. It is capable of reproducing complex failure modes that change from the matrix to the fibers depending on the type of stress state.

In contrast to most existing models for laminated composites, the model presented is of relatively simple numerical implementation in a nonlinear finite element program and it is able to reproduce nonlinear behavior of laminates. The model approximately reproduces the stiffness of the laminas and the failure of unidirectional laminas and composite laminates. The differences with experimental results are not greater than those obtained with the best-ranked models at the failure exercise [9–12].

Acknowledgment

The author wishes to thank the economical support of CONICET and CIUNT and Mrs. Amelia Campos for the English revision.

References

[1] Chaboche, J. L., Lesne, O., and Pottier, T., 1998, "Continuum Damage Mechanics of Composites: Towards a Unified Approach," *Damage Mechanics in Engineering Materials, Studies in Applied Mechanics 46*, Elsevier Voyiadjis, Ju and Chaboche, Elsevier, Vol. 46, pp. 3–26.

[2] Oller, S., Miquel, J., and Zalamea, F., 2005, "Composite Material Behavior Using a Homogenization Double Scale Method," J. Eng. Mech. Div., Am. Soc. Civ. Eng., **131**, pp. 65–79.

[3] Huang, Z., 2001, "Micromechanical Prediction of Ultimate Strength of Transversely Isotropic Fibrous Composites," Int. J. Solids Struct., **38**, pp. 4147–4172.

[4] Hinton, M. J., and Soden, P. D., 1998, "Predicting Failure in Composite Laminates: The Background to the Exercise," Compos. Sci. Technol., **58**, pp. 1001–1010.

[5] Soden, P. D., Hinton, M. J., and Kaddour, A. S., 1998, "Lamina Properties, Lay-Up Configurations and Loading Conditions for a Range of Fibre-Reinforced Composite Laminates," Compos. Sci. Technol., **58**, pp. 1011–1022.

[6] Hinton, M. J., Kaddour, A. S., and Soden, P. D., 2002, "Evaluation of Failure Prediction in Composite Laminates: Background to "Part B" of the Exercise," Compos. Sci. Technol., **62**, pp. 1481–1488.

[7] Soden, P. D., Hinton, M. J., and Kaddour, A. S., 2002, "Biaxial Test Results for Strength and Deformation of a Range of E-Glass and Carbon Fiber Reinforced Composite Laminates: Failure Exercise Benchmark Data," Compos. Sci. Technol., **62**, pp. 1489–1514.

[8] Hinton, M. J., Kaddour, A. S., and Soden, P. D., 2004, "Evaluation of Failure Prediction in Composite Laminates: Background to "Part C" of the Exercise," Compos. Sci. Technol., **64**, pp. 321–327.

[9] Soden, P. D., Hinton, M. J., and Kaddour, A. S., 1998, "A Comparison of the Predictive Capabilities of Current Failure Theories for Composite Laminates," Compos. Sci. Technol., **58**, pp. 1225–1254.

[10] Kaddour, A. S., Hinton, M. J., and Soden, P. D., 2004, "A Comparison of the Predictive Capabilities of Current Failure Theories for Composite Laminates: Additional Contributions," Compos. Sci. Technol., **64**, pp. 449–476.

[11] Hinton, M. J., Kaddour, A. S., and Soden, P. D., 2004, "A Further Assessment of the Predictive Capabilities of Current Failure Theories for Composite Laminates: Comparison with Experimental Evidence," Compos. Sci. Technol., **64**, pp. 549–588.

[12] Soden, P. D., Kaddour, A. S., and Hinton, M. J., 2004, "Recommendations for Designers and Researchers Resulting from the World-Wide Failure Exercise," Compos. Sci. Technol., **64**, pp. 589–604.

[13] Zinoviev, P., Grigoriev, S. V., Labedeva, O. V., and Tairova, L. R., 1998, "Strength of Multilayered Composites Under Plane Stress State," Compos. Sci. Technol., **58**, pp. 1209–1224.

[14] Zinoviev, P., Labedeva, O. V., and Tairova, L. R., 2002, "Coupled Analysis of Experimental and Theoretical Results on the Deformation and Failure of Laminated Composites Under a Plane State of Stress," Compos. Sci. Technol., **62**, pp. 11711–11724.

[15] Bogetti, T. A., Hoppel, C. P. R., Harik, V. M., Newill, J. F., and Burns, B. P., 2004, "Predicting the Nonlinear Response and Progressive Failure of Composite Laminates," Compos. Sci. Technol., **64**, pp. 477–485.

[16] Liu, K. S., and Tsai, S. W., 1998, "A Progressive Quadratic Failure Criterion of Alaminate," Compos. Sci. Technol., **58**, pp. 1023–3102.

[17] Kuraishi, A., Tsai, S. W., and Liu, K. A., 2002, "A Progressive Quadratic Failure Criterion Part B," Compos. Sci. Technol., **62**, pp. 1682–1696.

[18] Puck, A., and Schurmann, H., 1998, "Failure Analysis of FRP Laminates by Means of Physically Based Phenomenological Models," Compos. Sci. Technol., **58**, pp. 1045–1068.

[19] Puck, A., and Schurmann, H., 2002, "A Failure Analysis of FRP Laminates by Means of Physically Based Phenomenological Models—Part B," Compos. Sci. Technol., **62**, pp. 11633–11672.

[20] Cuntze, R. G., and Freund A, A., 2004, "The Predictive Capability of Failure Mode Concept-Based Strength Criteria for Multidirectional Laminates," Compos. Sci. Technol., **64**, pp. 343–377.

[21] Oller, S., Oñate, E., Miquel, J., and Botello, S., 1996, "A Plastic Damage Constitutive Model for Composite Materials," Int. J. Solids Struct., **33**(17), pp. 2501–2518.

[22] Luccioni, B., and López, D., 2002, "Modelo Para Materiales Compuestos Con Deslizamiento de Fibras," Análisis y *Cálculo de Estructuras de Materiales Compuestos*, CIME, Barcelona, España, Chap. 13 pp. 411–431.

[23] Luccioni, B., López, D., and Danesi, R., "Bond Slip in Reinforced Concrete Elements," J. Struct. Eng., ST/2002/023537, (in press).

[24] Betten, J., 1988, "Application of Tensor Functions to the Formulation of Yield Criteria for Anisotropic Materials," Int. J. Plast., **4**, pp. 29–46.

[25] Oller, S., Botello, S., Miquel, J., and Oñate, E., 1995, "An Anisotropic Elasto-Plastic Model Based on an Isotropic Formulation," Eng. Comput., **12**, pp. 245–262.

[26] Luccioni, B., Oller, S., and Danesi, R., 1995, "Plastic Damaged Model for Anisotropic Materials," Appl. Mech. Eng., **1**, pp. 124–129.

[27] Luccioni, B., Oller, S., and Danesi, R., 1996, "Coupled Plastic-Damaged Model," Comput. Methods Appl. Mech. Eng., **129**, 81–89.

[28] Car, E., Oller, S., and Oñate, E., 1999, "A Large Strain Plasticity Model for Anisotropic Material—Composite Material Application," Int. J. Plast., **17**(11), pp. 1437–1463.

[29] Oller, S., Car, E., and Lubliner, J., 2003, "Definition of a General Implicit Orthotropic Yield Criterion," Comput. Methods Appl. Mech. Eng., **192**, pp. 895–912.

[30] Luccioni, B., and Martín, P. E., 1997, "Modelo Elastoplástico Para Materiales Ortótropos," Rev. Int. Mét. Num. Dis, Cálc. Ing., **13**(4), pp. 603–614.

[31] Kriz, R. D., and Stinchomb, W. W., 1979, Exp. Mech., **19**, 41.

[32] Gundel, D. B., and Wawner, F. E., 1997, "Experimental and Theoretical Assessment of the Longitudinal Tensile Strength of Unidirectional SiC-Fiber/Titanium-Matrix Composites," Compos. Sci. Technol., **57**, pp. 471–481.

PROOF COPY [JAM-05-1183] 018605AMJ

AUTHOR QUERIES — 018605AMJ

#1 Au: Please check